High-Power 1180-nm GaInNAs DBR Laser Diodes

Antti T. Aho, Jukka Viheriälä, Ville-Markus Korpijärvi, Mervi Koskinen, Heikki Virtanen, Mathias Christensen, Topi Uusitalo, Kimmo Lahtonen, Mika Valden, and Mircea Guina

***Abstract*— We report high-power 1180-nm GaInNAs distributed Bragg reflector laser diodes with and without a tapered amplifying section. The untapered and tapered components reached room temperature output powers of 655 mW and 4.04 W, respectively. The diodes exhibited narrow linewidth emission with side-mode suppression ratios in the range of 50 dB for a broad range of operating current, extending up to 2 A for the untapered component and 10 A for the tapered component. The high output power is rendered possible by the use of a high quality GaInNAs-based quantum well gain region, which allows for lower strain and better carrier confinement compared with traditional GaInAs quantum wells. The development opens new opportunities for the power scaling of frequency-doubled lasers with emission at yellow–orange wavelengths.**

***Index Terms*— High power, distributed Bragg reflector lasers, frequency doubling, antireflection coatings.**

I. Introduction

LASERS emitting in the yellow–orange spectral range have many applications for example in dermatology [1], DNA sequencing [2], and spectroscopy [3]. However, this wavelength range cannot be reached directly with semiconductor lasers, which are the most practical and compact laser solutions whenever available. One viable approach for reaching the visible spectral range is frequency doubling from infrared (IR) laser radiation, which in turn, requires sources with high output power and narrow linewidth emission [4]. The frequency doubling scheme and the development of corresponding diodes with infrared emission has been vigorously addressed for blue–green spectral ranges where mature GaInAs quantum well (QW) gain materials can be used [4]. Several watts of green frequency-doubled radiation have been obtained using 1064 nm laser diodes [5]. However, the results for yellow frequency-doubled diodes have been more modest. This is largely due to the fact that it becomes increasingly difficult to reach high power close to 1.2 μm when using the standard materials. For example, using GaInAs QWs the maximum single-mode power obtained from untapered LDs at 1180 nm is about 230 mW [6] and about 3.2 W for tapered LDs [7]. Using quantum dots with an untapered design, a power of 80 mW has been reported [8]. As an alternative solution to achieve narrow linewidth emission in this wavelength range we have developed GaInNAs QWs and recently demonstrated an untapered distributed Bragg reflector laser diode (DBR-LD) emitting about 500 mW at 1180 nm and exhibiting a linewidth below 250 kHz over the entire operation range [9]. The addition of a small amount of nitrogen makes it possible to extend the wavelength range of the regular GaInAs QW and at the same time reduce the strain linked to In incorporation. Moreover, it also improves the carrier confinement resulting in improved temperature stability; in fact, we demonstrated a variation of the output power of only 30% for a temperature range extending from 20 °C to 80 °C [10].

In this letter we report further power scaling of the untapered 1180 nm DBR-LD with an output power as high as 655 mW at room temperature. Furthermore, by implementing a tapered design we demonstrate a room temperature output power of 4.04 W.

II. Laser Structure and Fabrication

The semiconductor structure was grown by plasma-assisted molecular beam epitaxy (MBE). The substrate was n-GaAs(100) and the active region comprised a single $Ga_{0.67}In_{0.33}N_{0.005}As$ QW. The QW was surrounded by a GaAs waveguide and $Al_{0.25}Ga_{0.75}As$ claddings. The semiconductor layers and the band gap structure are depicted in Fig. 1.

Compared to the previously reported structure [10], the In content of the QW was increased to shift the material gain to a longer wavelength, closer to the mode supported by the DBR grating. The photoluminescence wavelength of the wafer at room temperature was 1151 nm.

For the untapered design, the processed waveguide comprised a passive (unbiased), third-order DBR grating section with a length of 1.8 mm and an active ridge waveguide (RWG) section with a length of 2.9 mm. The DBR section selects a single longitudinal mode and the RWG section defines a single transversal mode. The width of both the DBR and the RWG was 3.2 μm.

Manuscript received August 28, 2017; revised September 21, 2017; accepted October 2, 2017. Date of publication October 6, 2017; date of current version October 30, 2017. This work was supported in part by the Academy of Finland under Grant 141481, in part by the FP7 Project RAPIDO under Grant 619806, in part by the H2020-ECSEL-2015 Project DENSE, in part by the HPY Research Foundation, in part by the Finnish Foundation for Technology Promotion, and in part by the KAUTE Foundation. *(Corresponding author: Antti T. Aho.)*

A. T. Aho, J. Viheriälä, M. Koskinen, H. Virtanen, T. Uusitalo, K. Lahtonen, M. Valden, and M. Guina are with the Optoelectronic Research Centre, Tampere University of Technology, 33101 Tampere, Finland (e-mail: antti.t.aho@tut.fi; jukka.viheriala@tut.fi; mervi.koskinen@tut.fi; heikki.a.virtanen@tut.fi; topi.uusitalo@tut.fi; kimmo.lahtonen@tut.fi; mika.valden@tut.fi; mircea.guina@tut.fi).

V.-M. Korpijärvi was with the Optoelectronic Research Centre, Tampere University of Technology, 33101 Tampere, Finland. He is now with Okmetic Oyj, 01301 Vantaa, Finland (e-mail: ville.korpijarvi@hotmail.com).

M. Christensen is with Norlase ApS, DK-4000 Roskilde, Denmark, and also with the Department of Photonics Engineering, Technical University of Denmark, DK-4000 Roskilde, Denmark (e-mail: mac@norlase.com).

Color versions of one or more of the figures in this letter are available online at http://ieeexplore.ieee.org.

Digital Object Identifier 10.1109/LPT.2017.2760038

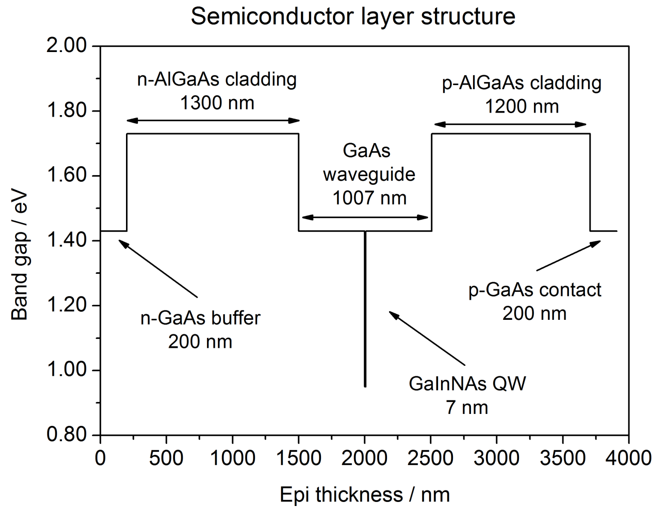

Fig. 1. Semiconductor layer structure revealing the band gap profile.

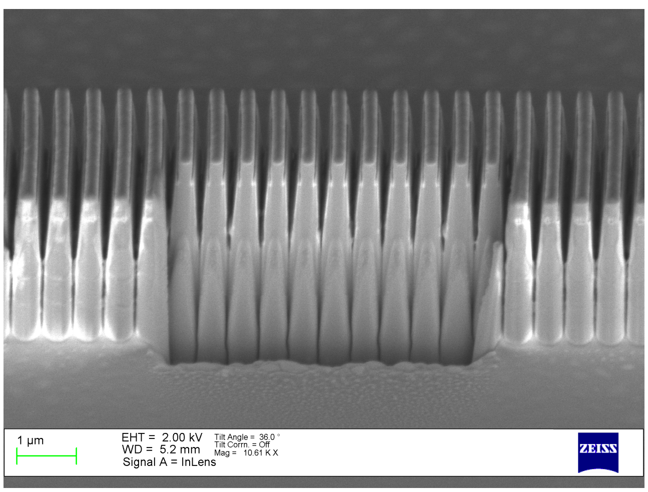

Fig. 2. Scanning electron microscope picture of the grating side profile. Focused ion beam (FIB) has been used to cut into the grating in order to better see the cross-section in the middle.

The grating and the ridge were fabricated without regrowth, using low-cost and high-throughput soft-stamp ultraviolet nanoimprint lithography [11]. The basic fabrication steps of the gratings have been presented in [10]. In this work, the side profile of the grating was tuned by adjusting the etching recipe in order to reach a grating filling factor of approximately 0.85 leading to a higher reflection coefficient and lower radiative losses [12]. The etching was performed using Cl_2/N_2-based inductively coupled plasma reactive ion etching (ICP-RIE). The etching depths of the grating and the RWG were 1200 nm and 1350 nm, respectively. The achieved grating side profile can be seen in Fig. 2.

The design of the tapered DBR-LD comprises a 2 mm long passive DBR section, a 1 mm long active RWG section and a 4 mm long gain-guided tapered amplifying section with a tapering angle of 5°. The DBR and RWG widths were 3.2 μm, and the DBR and RWG etching depths were 1500 nm and 1350 nm, respectively.

The components were packaged by first soldering the chips p-side down on ceramic AlN submounts with AuSn solder and then bonding the submounts on gold plated copper heatsinks with indium solder. The chips were antireflection (AR) coated to suppress unwanted Fabry-Perot operation and to improve the outcoupling from the front facet. Traditionally thin-film AR coatings have been prepared by methods such as electron beam and thermal evaporation, ion assisted deposition, ion beam sputtering, or magnetron sputtering. In the work presented here, atomic layer deposition (ALD) was used as an alternative method to fabricate the AR coatings on laser facets. A two-layer Al_2O_3 (128.7 nm)/TiO_2 (77.6 nm) AR design was fabricated on the untapered component and a single-layer Al_2O_3 (146.8 nm) design on the tapered component using Picosun Sunale ALD R200 Advanced reactor. The two-layer and single-layer coatings were grown at substrate temperatures of 100 °C and 200 °C, respectively. Trimethylaluminium, tetrakis-(dimethylamino)titanium, and deionized water were used as precursors. At 100 °C, refractive indices of 1.595 and 2.401 were determined for Al_2O_3 and TiO_2 layers, respectively. The refractive index of Al_2O_3 grown at 200 °C was determined to be 1.665. The performance of the AR coatings was assessed using reference substrates and reflectance spectroscopy with Perkin Elmer Lambda 1050 UV/Vis/NIR Spectrophotometer. The ALD growth processes yielded an Al_2O_3/TiO_2 two-layer thin film and an Al_2O_3 single-layer thin film with reflectances below 1% and approximately 3% at 1180 nm, respectively.

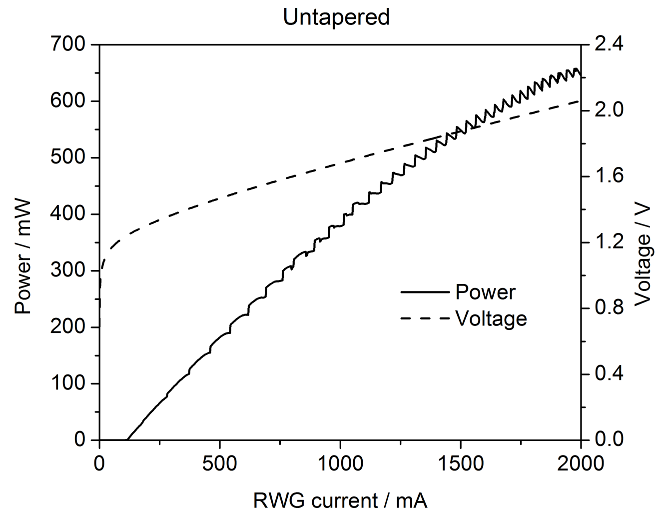

Fig. 3. The output power and voltage of the untapered LD from 0 mA to 2000 mA at 20 °C.

III. RESULTS

The CW ILV (current, power, voltage) characteristics of an untapered and tapered DBR-LD at 20 °C mount temperature are shown in Fig. 3 and Fig. 4, respectively. The untapered component was measured up to a current of 2 A and the tapered component up to a taper current (I_{TA}) of 10 A with a constant 350 mA RWG injection current (I_{RWG}). The kinks in the untapered component output power are related to the lasing longitudinal mode changing to match the maximum DBR reflectivity, when the temperature of the active

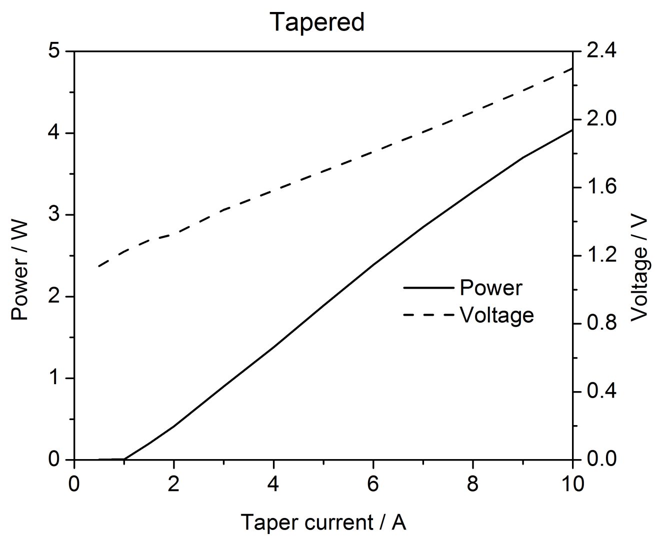

Fig. 4. The output power and voltage of a tapered LD from 0 A to 10 A tapered section current at 20 °C. The RWG section current was held at constant 350 mA.

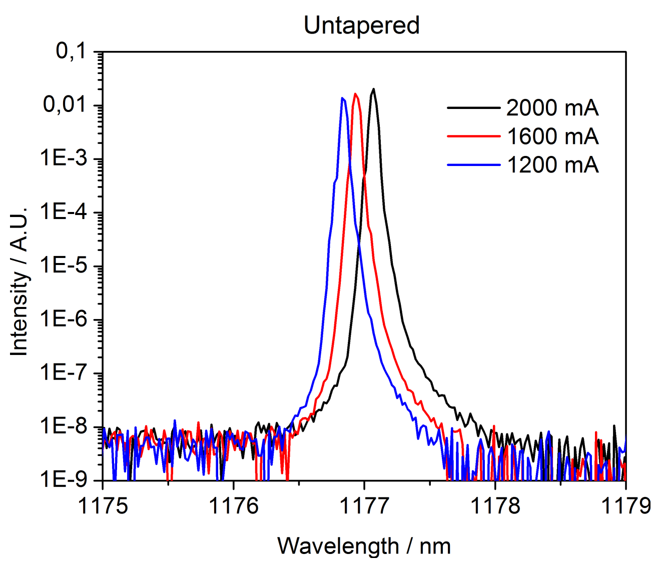

Fig. 5. Spectra from the untapered component at 20 °C mount temperature with various injection currents. The spectral resolution is 0.05 nm.

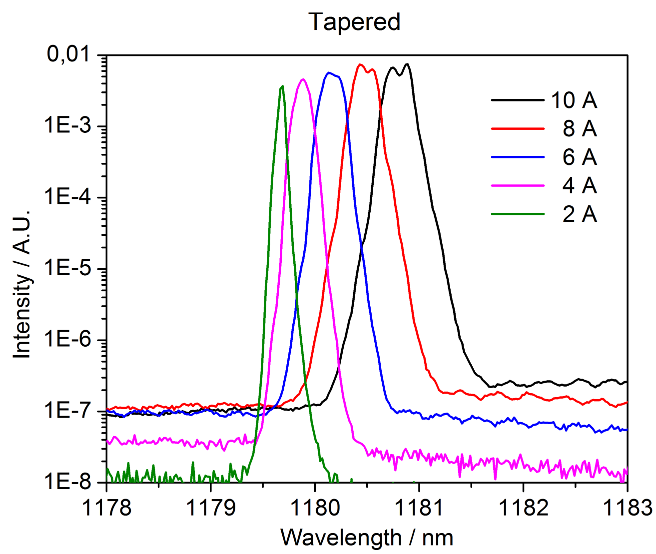

Fig. 6. Spectra from the tapered component at 20 °C mount temperature with various I_{TA} while I_{RWG} was constant 350 mA. The spectral resolution is 0.05 nm.

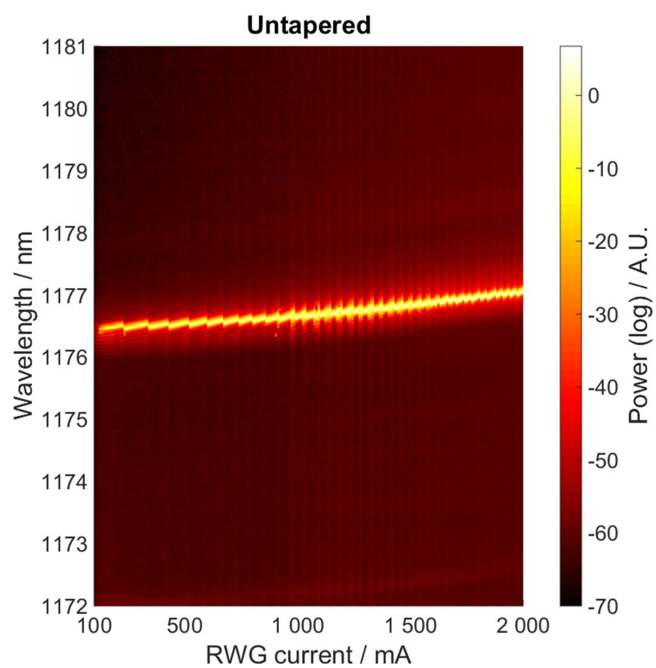

Fig. 7. Spectra of the untapered component from 100 mA to 2000 mA.

region increases [13]. At 20 °C the untapered and tapered components reached output powers of about 655 mW and 4.04 W, respectively (limited by the current range used for the measurements). We note that the power curve for the tapered LD does not show significant signs of roll-off at the maximum current available for the measurement.

The emission wavelength of the components could be tuned by changing the mount temperature or the injection current. The tuning rates for the untapered and tapered components were about 90 pm/°C for temperature and about 0.30 pm/mA and 0.14 pm/mA for current, respectively. The emission spectra with various injection currents are shown in Fig. 5 and Fig. 6. The mode hops between adjacent DBR modes and the shift in the emission wavelength with increasing current can be seen in Fig. 7 and Fig. 8. The temperature stability of the components was good: the untapered and tapered components reached output powers of over 400 mW and over 1500 mW at 60 °C, respectively.

The spectrum full width at half maximum (FWHM) at 20 °C mount temperature was 50 pm for the untapered component with 2000 mA injection current and 270 pm for the tapered component with $I_{TA} = 10$ A, $I_{RWG} = 350$ mA. The spectral width of the untapered component was limited by the resolution of the used Anritsu MS9710C optical spectrum analyzer [14], but self-homodyne linewidth measurements from previous generation components with similar structure have yielded fitted Lorentzian FWHM below 250 kHz [9].

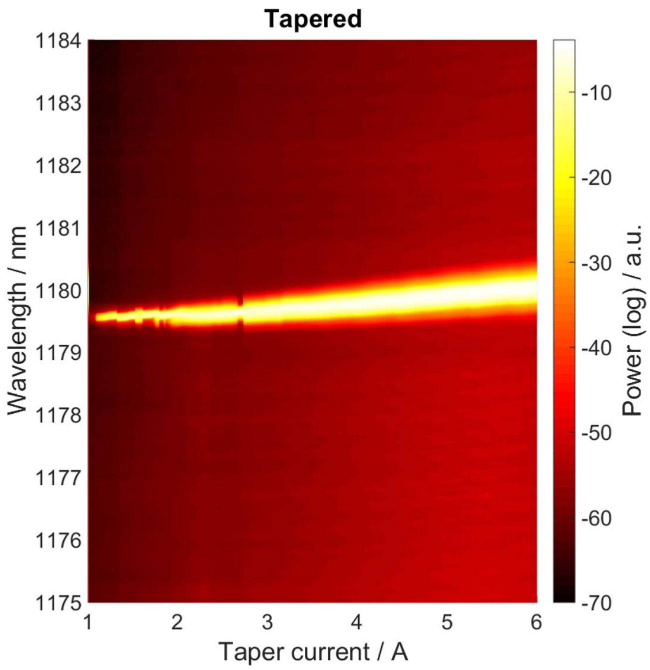

Fig. 8. Spectra of the tapered component from 1 A to 6 A with $I_{RWG} = 350$ mA.

We expect that the FWHM of the tapered component can be significantly reduced by using an AR coating with a smaller reflectance. A preliminary test showed that, at a power level of 1.7 W, applying a two-layer Al_2O_3/TiO_2 AR coating to a tapered DBR (similar to the coating we applied to the untapered DBR) resulted in a spectral peak FWHM of 70 pm, which is close to the resolution limit of the spectrum analyzer, while the single-layer Al_2O_3 AR coating resulted in a FWHM of 220 pm.

The far-field (FF) fast axis and slow axis FWHM of the untapered component at 2000 mA injection current were $\sim 40°$ and $\sim 7°$, respectively. For the tapered component at 10 A injection current, the FF fast axis and slow axis FWHM were $\sim 40°$ and $\sim 6°$, respectively.

IV. Conclusions

We reported the highest power to date for narrow-linewidth untapered DBR laser diodes emitting around 1180 nm and demonstrated for the first time GaInNAs tapered DBR laser diodes in this wavelength range. At room temperature the output power of the untapered and tapered DBR-LDs reached 655 mW and 4.04 W, respectively. The high output power is linked to the use of a GaInNAs-based QW structure which enables smaller strain and improved carrier confinement compared to traditional GaInAs material. The high output power and narrow linewidth make these kinds of components interesting for the development of frequency-doubled lasers with emission at yellow–orange wavelengths.

References

[1] N. S. Sadick and R. Weiss, "The utilization of a new yellow light laser (578 nm) for the treatment of Class I red telangiectasia of the lower extremities," *Dermatolic Surg.*, vol. 28, no. 1, pp. 21–25, Jan. 2002.

[2] K. M. Murray, "DNA sequencing by mass spectrometry," *J. Mass Spectrometry*, vol. 31, no. 11, pp. 1203–1215, Nov. 1996.

[3] T. Nishikawa, A. Ozawa, Y. Nishida, M. Asobe, F. Hong, and T. W. Hänsch, "Efficient 494 mW sum-frequency generation of sodium resonance radiation at 589 nm by using a periodically poled Zn:$LiNbO_3$ ridge waveguide," *Opt. Exp.*, vol. 17, no. 20, pp. 17792–17800, 2009.

[4] A. Jechow, R. Menzel, K. Paschke, and G. Erbert, "Blue-green light generation using high brilliance edge emitting diode lasers," *Laser Photon. Rev.*, vol. 4, no. 5, pp. 633–655, Sep. 2010.

[5] A. K. Hansen *et al.*, "Concept for power scaling second harmonic generation using a cascade of nonlinear crystals," *Opt. Exp.*, vol. 23, no. 12, pp. 15921–15934, 2015.

[6] K. Paschke *et al.*, "Watt-level continuous-wave diode lasers at 1180 nm with InGaAs quantum wells," in *Proc. SPIE*, 2014, p. 896509. [Online]. Available: http://dx.doi.org/10.1117/12.2037752

[7] R. Bege *et al.*, "Watt-level second-harmonic generation at 589 nm with a PPMgO:LN ridge waveguide crystal pumped by a DBR tapered diode laser," *Opt. Lett.*, vol. 41, no. 7, pp. 1530–1533, 2016.

[8] J. Koeth, M. Fischer, M. Legge, J. Seufert, and R. Werner, "High performance quantum dot distributed feedback laser diodes around 1.15 μm," in *Proc. SPIE*, 2008, p. 690904. [Online]. Available: http://dx.doi.org/10.1117/12.763157

[9] H. Virtanen *et al.*, "Spectral characteristics of narrow-linewidth high-power 1180 nm DBR laser with surface gratings," *IEEE Photon. Technol. Lett.*, vol. 29, no. 1, pp. 114–117, Jan. 1, 2017.

[10] V.-M. Korpijärvi, J. Viheriälä, M. Koskinen, A. T. Aho, and M. Guina, "High-power temperature-stable GaInNAs distributed Bragg reflector laser emitting at 1180 nm," *Opt. Lett.*, vol. 41, no. 4, pp. 657–660, 2016.

[11] J. Viheriälä *et al.*, "Applications of UV-nanoimprint soft stamps in fabrication of single-frequency diode lasers," *Microelectron. Eng.*, vol. 86, no. 3, pp. 321–324, Mar. 2009.

[12] H. Wenzel, R. Guther, A. M. Shams-Zadeh-Amiri, and P. Bienstman, "A comparative study of higher order Bragg gratings: Coupled-mode theory versus mode expansion modeling," *IEEE J. Quantum Electron.*, vol. 42, no. 1, pp. 64–70, Jan. 2006.

[13] M. Achtenhagen, N. V. Amarasinghe, and G. A. Evans, "High-power distributed Bragg reflector lasers operating at 1065 nm," *Electron. Lett.*, vol. 43, no. 14, pp. 755–757, Jul. 2007.

[14] *MS9710C Optical Spectrum Analyzer Operation Manual*, 11th ed. Atsugi, Japan: Anritsu Corporation, 2008.